Supplemental Material and Methods

Detailed Methods

Animals

All animal experimental procedures were approved by the Airforce Medical University Animal Use and Care Committee. Eight-week-old male C57BL/6J mice were purchased from Shanghai Biomodel Organism Science & Technology Development Lab. Conditional cardiac-specific Dlat transgenic mice were generated with an LSL cassette under the control of a proximal CAG promoter followed by Dlat cDNA. Briefly, CAG-LSL-Dlat-IRES-tdTomato-WPRE-polyA expression cassette were inserted at the site of Rosa26 gene through homologous recombination. Activation of αMyHC-Cre recombinase enable deletion of the floxed STOP cassette, thereby allowing conditional expression of Dlat in cardiomyocytes. Resultant Tg (CAG-LSL-Dlat-IRES-tdTomato-WPRE-polyA) Cre+/- transgenic mice ($Dlat^{Tg}$) were used for the experiments. Littermates without Cre-induced recombination were used as a control ($Dlat^{NTg}$). Tamoxifen was intraperitoneally injected at 4-weeks of age to induce Cre activity. All mice were housed in a temperature-, humidity-, and light-controlled room and allowed free access to water and food.

HFpEF constructed by a 2-Hit strategy

The HFpEF model was induced with a 2-hit strategy as previously reported[1]. Briefly, 8-week-old mice were fed with a combination of high-fat diet (HFD, Research Diets, #D12492) and L-NAME (Nω-nitrol-arginine methyl ester; 0.75 g/L; N5751, Sigma Aldrich) in the drinking water for 15 weeks. Control mice were fed with a chow-diet. Nicotinamide Riboside (NR) was custom synthesized by Shanghai Macklin Biotechnology Co., Ltd. (Shanghai, China) as previously described[2]. Mice were each given NR via daily oral gavage at a dose of 400mg/kg/d. For oral spermidine (SPD) supplementation, SPD (Sigma-Aldrich, S4139) was administered *per os* in drinking water at a final concentration of 30 mM. To avoid excessive deamination of the active compound, water with NR or SPD was replaced three times a week.

Measurement of blood glucose and serum lipid level

Mice blood was collected after overnight fast. Blood glucose was measured using a glucometer (Yuwell, China). Low density lipoprotein (LDL)-cholesterol, high-density lipoprotein (HDL)-cholesterol and triglycerides were detected by clinical laboratory of Tangdu Hospital using a Chemray800 automatic biochemical analyzer (Rayto, Shenzhen, China) with standard protocol.

Down-regulation and up-regulation of target genes

Empty adenoviral vectors (Ad-NC), adeno-associated virus 9 expressing Dlat-specific small hairpin RNA (AAV-9 Dlat-shRNA), adeno-associated virus 9 expressing HADHA (AAV-9 HADHA), and recombinant adenoviral vectors expressing Dlat (Ad-Dlat), were conducted by Hanbio Biotechnology Ltd (Shanghai, China). For adenovirus transfection, cardiomyocytes were incubated in Opti-MEM (Invitrogen) containing adenovirus (MOI: 50/1) for 6-8 h.

Echocardiographic assessment

Echocardiographic assessment was performed with a Vevo 3100 echocardiography instrument (Visual sonics, Canada) and VINNO 10 echocardiography instrument (Vinno, China) as previously described. Briefly, mice were anesthetized with 2% isoflurane and maintained under anesthesia with 1.5% isoflurane. Ejection fraction (EF%) and fraction shortening (FS%) was determined from long-axis M-modes. d. Doppler echocardiography was obtained to determine diastolic trans-mitral blood flow velocities for peak early (E) and late (A) fillings.

Glucose tolerance test

An intraperitoneal glucose tolerance test (IPGTT) was performed after overnight fasting. Mice were intraperitoneally injected with glucose(2g/kg). Blood glucose was measured at 0-, 15-, 30-, 60-, 90-, and 120-min using tail clippings.

Exercise performance

Exercise performance was determined with run to exhaustion treadmill testing. For run to exhausting treadmill testing, mice were motivated on a treadmill and considered

exhausted when they could no longer run in response to electronic stimulus. The speed of run protocol was started at 10m/min for 10min. Then, the speed was increased in 2-m/min increments every 10 min until exhaustion. The run distance was recorded.

Isolation of mouse heart mitochondria

Cardiac tissues were surgically removed and immediately placed in ice-chilled MSE buffer (70 mM sucrose, 210 mM mannitol, 5 mM MOPS, 2 mM taurine, 1.6 mM carnitine hydrochloride, and 1 mM EDTA, pH 7.4) to remove residual blood. The specimens were then mechanically dissected into fragments in precooled MSE buffer (4°C). Following initial low-speed centrifugation (600g, 5 min), the processed tissue was reconstituted in MSE solution containing 0.1 mg/mL trypsin for 10-minute ice incubation. To counteract trypsin activity, an equivalent volume of MSE buffer supplemented with 0.2% fatty acid-free BSA and 0.5 mg/mL trypsin inhibitor was added under chilled conditions. After subsequent medium-speed centrifugation (1500g, 3 min), the cellular material was dispersed in 4 mL of BSA-containing MSE buffer (0.2%) using a glass Dounce homogenizer (6 cycles at 1200 rpm). The lysate underwent two-phase clarification: initial debris removal through 600g centrifugation (5 min) followed by supernatant transfer for high-speed processing (8000g, 10 min). The collected biological sediment underwent washing repetition (8000g, 10 min) before final resuspension in 150 μL MSE buffer for mitochondrial isolation.

Measurement of Mitochondria Respiration in Heart Lysates

High-resolution respirometry was performed using an Oxygraph-2K system (Oroboros Instruments). The apparatus underwent temperature-controlled standardization (37°C) for 60 minutes using MiR05 equilibration medium containing (in mM): 500 EGTA, 3 $MgCl_2 \cdot 6H_2O$, 60 K-lactobionate, 20 taurine, 10 KH_2PO_4, 20 HEPES, 110 sucrose, supplemented with 1g/L fatty acid-free BSA (pH 7.1, KOH-adjusted). Continuous stirring (540 rpm) maintained dissolved oxygen stability until air-saturation equilibrium was confirmed through stabilized O_2 flux readings. Cardiac specimens (~5 mg wet mass) underwent cryopreserved mechanical disruption in chilled MiR05 medium. Resultant lysates were transferred to temperature-regulated 2 mL measurement chambers for real-

time oxygen consumption monitoring. Fatty acid metabolic capacity was determined through sequential addition of 5 mM ADP, 2 mM malate, and 0.5 mM octanoylcarnitine (Oct) to initiate palmitoyl-carnitine dependent respiration.

Measurement of mitochondrial respiration and glycolysis in NRVCMs

The Seahorse XFe96 Analyzer (Agilent Technologies) was employed for real-time measurement of oxygen consumption rate (OCR) and extracellular acidification rate (ECAR). Sensor cartridges were hydrated overnight at 37°C in 200 μL XF Calibrant Solution (pH 7.4) under non-CO_2 conditions. NRVCMs were maintained in were seeded into XFe96 cell culture microplates and incubated for 24 h. Quadruplicate wells containing culture medium without cells served as background controls. Mitochondrial respiration was measured with 1.5 μM oligomycin, 2.0 μM FCCP and 0.5 μM rotenone + 0.5 μM antimycin A. ECAR were measured with ECAR 10 mM glucose, 1.0 μM oligomycin and 50 mM 2-deoxy-D-glucose. For fatty acid oxidation measurement, palmitate was added into the solution while etomoxir were employed to inhibit fatty acid oxidation.

Isolation of Adult Mouse Cardiomyocytes

The isolation of adult cardiomyocytes was performed through retrograde coronary perfusion in anesthetized and heparinized murine models. Following median sternotomy, excised hearts were immediately transferred to oxygenated perfusion buffer (37°C, pH 7.2, 5% CO_2-95% O_2) and cannulated via the aortic arch under stereomicroscopic guidance for continuous coronary perfusion at 2.2 ml/min using modified Joklik's MEM supplemented with 1.2 mM $MgSO_4$, 1.0 mM dl-carnitine, and 23.8 mM $NaHCO_3$. After 10-minute stabilization, enzymatic digestion was initiated by recirculating the perfusion medium containing 150 U/mL collagenase II and 0.1% fatty acid-free BSA until tactile confirmation of myocardial softening. The softened cardiac tissue was dissected in dissociation buffer (Joklik's MEM with 0.8% BSA and 0.75 mM $CaCl_2$), followed by mechanical fragmentation of the left ventricle into 5 mm segments and orbital shaking incubation (100 rpm, 37°C) in collagenase/BSA solution for 15-20 minutes under carbogen atmosphere. The resultant cell suspension underwent

sequential purification through 250 μm mesh filtration and differential centrifugation (600g, 45 sec, 21°C) in isotonic HEPES-based solution (135 mM NaCl, 5 mM KCl, 1 mM $MgCl_2 \cdot 6H_2O$, 1.2 mM $CaCl_2 \cdot 2H_2O$, 10 mM HEPES, 8 mM glucose), with supernatant removal and buffer replacement ensuring cardiomyocyte enrichment while eliminating cellular debris.

Acetylome profiling

For acetylome profiling analysis, proteins were extracted using urea-Tris buffer (8 M urea, 100 mM Tris/HCl, pH 8.5), quantified via Bradford assay, and separated by SDS-PAGE (12.5% gel). In-solution digestion included DTT reduction (10 mM, 37°C), IAA alkylation (50 mM), and trypsin cleavage (1:50 ratio, 37°C overnight). Peptides were desalted (C18 cartridges) and lyophilized. Acylated peptides were enriched using PTMScan® antibody-conjugated beads (Cell Signaling Technology), followed by elution with 0.15% TFA and desalting (C18 STAGE tips).LC-MS/MS analysis (timsTOF Pro, Bruker) utilized a C18 column (25 cm × 75 μm, 1.9 μm) with a 60-min acetonitrile gradient (0.1% formic acid). MS parameters: m/z 100–1700, PASEF MS/MS (10 cycles), and ion mobility (1/k0 0.6–1.6). Data were processed via MaxQuant (UniProt database, 1% FDR) with fixed (carbamidomethylation) and variable modifications (oxidation, acylations). Bioinformatics included hierarchical clustering (Cluster 3.0), motif analysis (MEME), subcellular localization (CELLO), functional annotation (GO/KEGG), enrichment (Fisher's test, $p < 0.05$), and PPI networks (STRING/Cytoscape).

RNA Extraction and Quantitative Real-Time Polymerase Chain Reaction

Total RNA was isolated from NRVCMs or cardiac tissue using TRIzol reagent (Takara), where samples were mechanically disrupted in ice-cold TRIzol followed by chloroform-mediated phase separation. The aqueous phase containing RNA was mixed with isopropyl alcohol for precipitation, washed with 75% ethanol, and resuspended in RNase-free water. RNA purity and concentration were determined spectrophotometrically (NanoDrop 2000, Thermo Scientific) with acceptable A260/A280 ratios between 1.8-2.1. Genomic DNA contamination was eliminated

through DNase I treatment (Ambion) at 37°C for 30 min, followed by RNA purification using silica-membrane columns (RNeasy Mini Kit, Qiagen). First-strand cDNA synthesis was performed with 1 μg total RNA using oligo(dT) primers and M-MLV reverse transcriptase (Promega) under thermal cycling conditions: 25°C for 5 min, 42°C for 60 min, and 70°C for 15 min. Quantitative PCR amplification was conducted in triplicate using SYBR Green Master Mix (Applied Biosystems) on a CFX96 Real-Time PCR Detection System (Bio-Rad), with reaction parameters set as: initial denaturation at 95°C for 3 min, followed by 40 cycles of 95°C for 15 sec and 60°C for 30 sec. Melt curve analysis (65-95°C, 0.5°C increments) confirmed primer specificity. Gene expression was normalized to β-actin and quantified via the comparative ΔΔCt method, with amplification efficiencies (90-110%) validated through standard curve analysis using serial cDNA dilutions. The sequences of primers used are the following: Nppa forward primers: 5′-CTCCGATAGATCTGCCCTCTTGAA-3′ and reverse: 5'-GGTACCGGAAGCTGTTGCAGCCTA-3'; β-MHC forward primers: 5'-CAGACATAGAGACCTACCTTC-3' and reverse was 5'-CAGCATGTCTAGAAGCTCAGG-3'. Nppb forward primer, 5'-AAGCTGCTGGAGCTGATAAGA-3'; reverse primer, 5'-GTTACAGCCCAAACGACTGAC3'.

Immunoblot Analysis

Mice heart and NRVCMs were analyzed by western-blotting as previously described[2]. Primary antibodies against the following proteins were used: CD36 (Abcam, #ab252922), HADHA (Abcam, #ab54477), HADHB (Abcam, # ab230667), Cpt1b (Abcam, #ab134988), CrAT (Proteintech, #15170-1-AP), Acadl (Abcam, # ab129711), Dlat (Abcam, # ab172617), SIRT3 (Abcam, # ab217319), IDH2 (Proteintech, #66918-1-Ig), OGDH (Abcam, # ab137773), HK2(Proteintech, #66974-1-Ig), PFK1(Proteintech, #55028-1-AP), PKM2(Proteintech, #60268-1-Ig), LDHA (Abcam, #ab52488), Acetylated-Lysine(Cell signaling technology, #9441), Flag (Proteintech, #20543-1-AP), Actin (Proteintech, #66009-1-Ig), GAPDH (Proteintech, #60004-1-Ig), VDAC1(Proteintech, #55259-1-AP).

Lipodomics

Cardiac lipid extraction was performed on snap-frozen murine heart tissue samples using methyl-tert-butyl ether/methanol/water biphasic solvent system with 10 μL SPLASH LipidoMix internal standard (Avanti Polar Lipids). Tissue homogenates were vortexed, sonicated, and centrifuged to isolate lipid-containing organic phase. Lipid species were analyzed via ultra-high-performance liquid chromatographycoupled with Q-Exactive HF-X Hybrid Quadrupole-Orbitrap mass spectrometer, employing C18 column with gradient elution. Data-dependent acquisition (DDA) operated in both positive/negative ionization modes with dynamic exclusion. Lipid identification utilized LipidSearch 4.2 software (Thermo Scientific) against LIPID MAPS database, applying mass accuracy and retention time alignment. Quantitation normalized to internal standards and tissue weight, with multivariate analysis including orthogonal partial least squares-discriminant analysis for group discrimination. Quality control pooled samples injected every 10 runs ensured instrumental stability. Differential lipids (VIP >1.0, $p<0.05$, FDR-adjusted) were annotated via MS/MS spectral matching and confirmed against authentic standards when available.

HADHA activity measurement

HADHA enzymatic activity was determined in total heart lysates or cell lysates as previously described[3]. Briefly, cell or heart lysates were added into a 96-well plate. The reaction system of 190 μL was constructed by adding 160 μL of 50 mM imidazole and 20 μL of 1.5 mM NADH. The reaction was initiated by the addition of 10 mL of 2 mM acetoacetyl CoA. A spectrophotometer kinetic plate reader was used to follow the absorbance at a 340 nm wave length.

Reference:

1. Schiattarella GG, Altamirano F, Tong D, French KM, Villalobos E, Kim SY, Luo X, Jiang N, May HI, Wang ZV, et al. Nitrosative stress drives heart failure with preserved ejection fraction. *Nature*. 2019;568:351-356. doi: 10.1038/s41586-019-1100-z
2. Hu L, Guo Y, Song L, Wen H, Sun N, Wang Y, Qi B, Liang Q, Geng J, Liu X, et al. Nicotinamide riboside promotes Mfn2-mediated mitochondrial fusion in diabetic hearts through the SIRT1-PGC1α-PPARα pathway. *Free Radic Biol Med*. 2022;183:75-88. doi: 10.1016/j.freeradbiomed.2022.03.012
3. Chi Z, Chen S, Xu T, Zhen W, Yu W, Jiang D, Guo X, Wang Z, Zhang K, Li M, et al.

Histone Deacetylase 3 Couples Mitochondria to Drive IL-1β-Dependent Inflammation by Configuring Fatty Acid Oxidation. *Mol Cell*. 2020;80:43-58.e47. doi: 10.1016/j.molcel.2020.08.015

Supplemental Figures and Figures legends

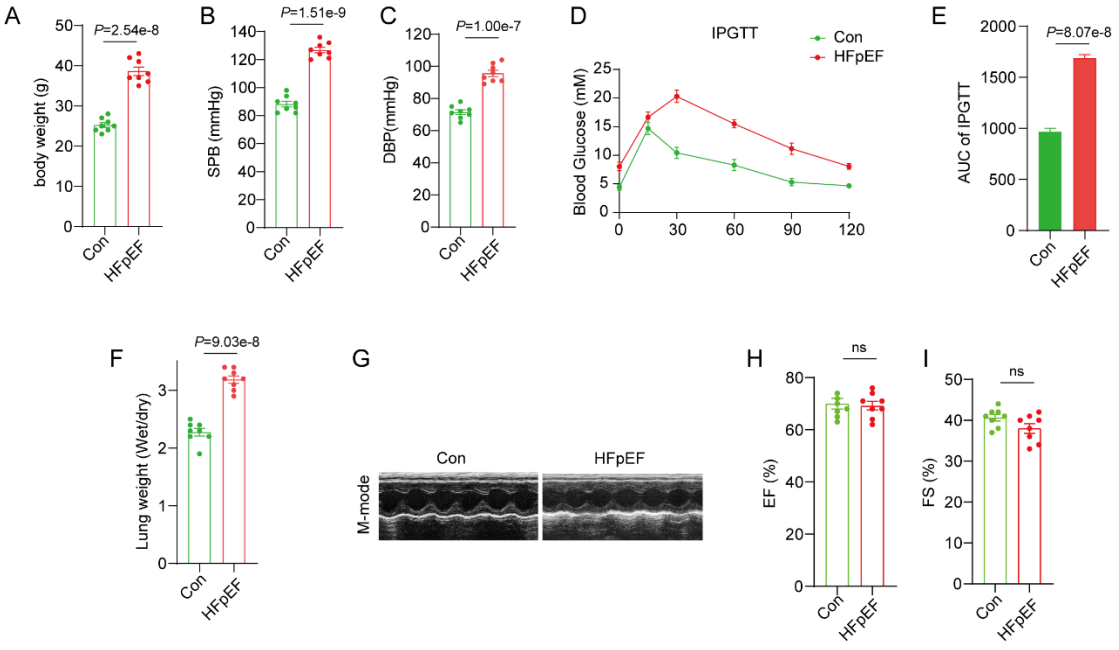

FigS1 Systemic comorbidities, cardiac systolic function, and glucose hemostasis in HFpEF mice. A, Body weight of Control and HFpEF mice were measured; **B-C,** Systolic blood pressures (SBP) and diastolic blood pressures(DBP) were recorded using a pressure transducer (AD Instruments); **D,** Intraperitoneal glucose tolerance test (IPGTT) was performed after 16 hours of fasting by injecting sterile 20% dextrose (2 g/kg) intraperitoneally; **E,** AUC of glucose levels from 0 to 120 min; **F,** The ratio of wet-to-dry lung weight was using to assess pulmonary congestion; **G-I,** Left Ventricular Ejection Fraction(LVEF) and left ventricular fractional shortening (LVFS) values were measured using echocardiography to assess left ventricular systolic function. Data presented as mean ± SEM; each point represents an individual animal; Statistical Analysis based on the Student's t-test. HFpEF indicates heart failure with preserved ejection fraction model induced by the 2-hit strategy.

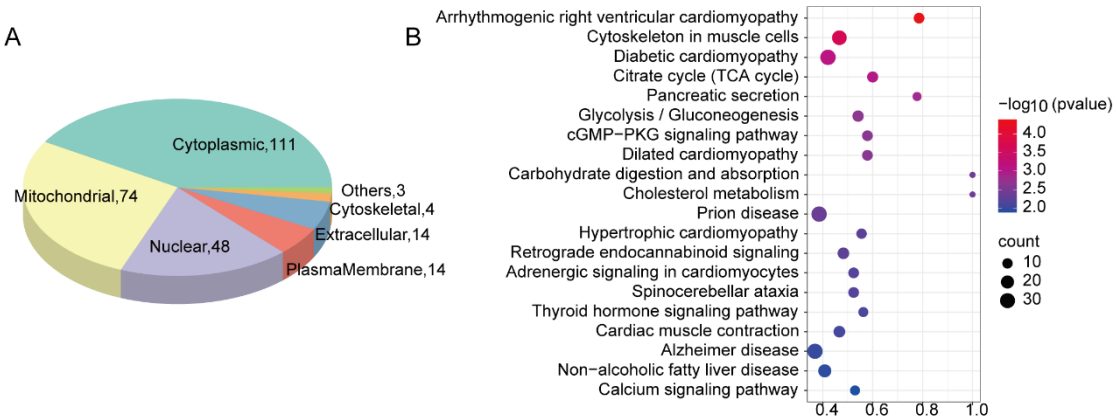

FigS2 Down-regulated acetylated proteins in the HFpEF hearts were analyzed by acetylome profiling.

A, Subcellular distribution of the down-regulate acetylated proteins in HFpEF hearts (n=3 mice per group); **B,** Kyoto Encyclopedia of Genes and Genomes (KEGG) enrichment analysis of the down-acetylated proteins in the HFpEF hearts.

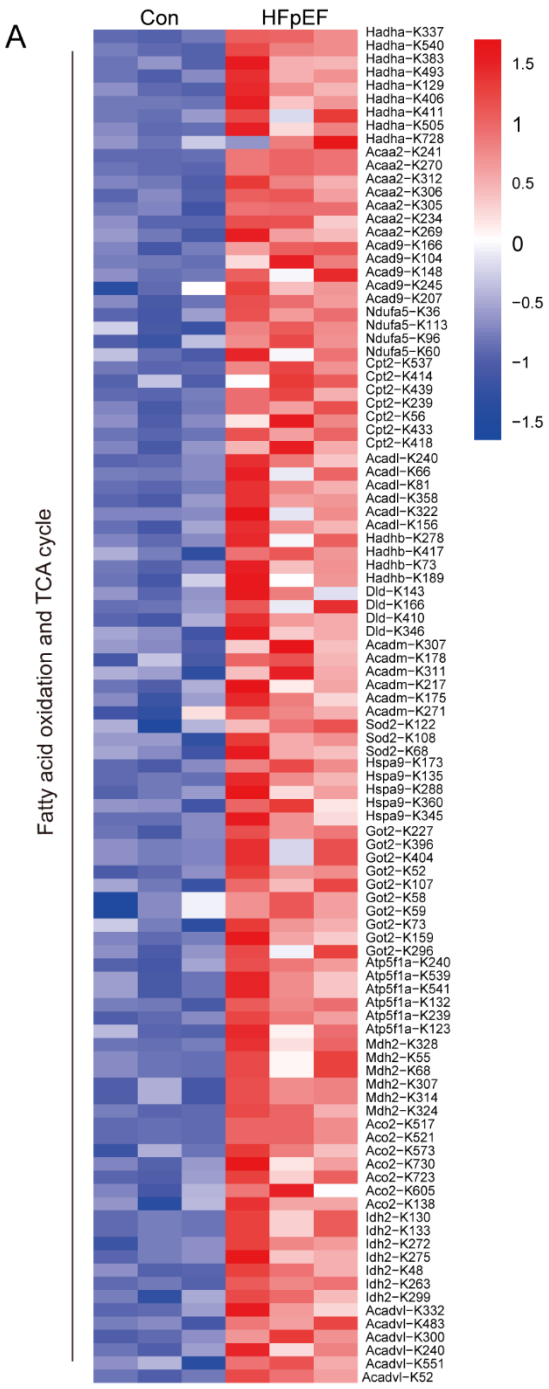

FigS3, **Main proteins involved in TCA cycles and fatty acid oxidation were hyperacetylated in the HFpEF hearts.**

A, Heatmap showing the acetylation levels of peptides mapping to TCA cycle and fatty acid oxidation in HFpEF heart as compared to Control group (n=3 mice per group).

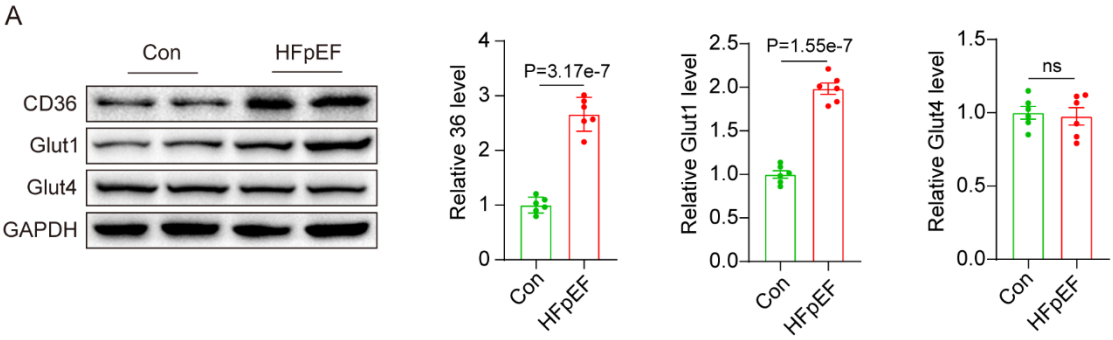

FigS4 Expression of CD36, Glut1 and Glut4 were determined in the HFpEF hearts. **A,** Immunoblot analysis and quantification of CD36, Glut1 and Glut4 from the control and HFpEF hearts. Data presented as mean ± SEM; each point represents an individual animal; Statistical Analysis based on the Student's t-test. HFpEF indicates heart failure with preserved ejection fraction model induced by the 2-hit strategy.

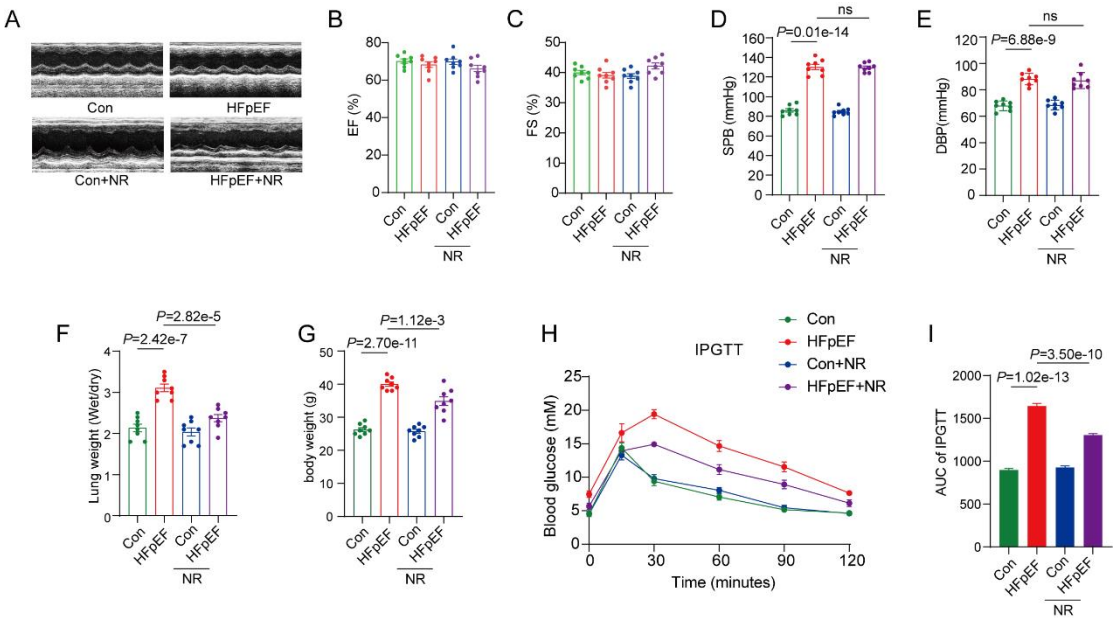

FigS5 Impact of NR supplementation on systemic comorbidities, cardiac systolic function, and glucose hemostasis in HFpEF mice.

A-C, Left Ventricular Ejection Fraction(LVEF) and left ventricular fractional shortening (LVFS) values were measured using echocardiography to assess left ventricular systolic function; **D-E,** Systolic blood pressures (SBP) and diastolic blood pressures(DBP) were recorded using a pressure transducer (AD Instruments); **F,** Pulmonary congestion was assessed by the ratio of wet-to-dry lung weight; **G,** Body weight of male C57BL/6 mice in the control, HFpEF, control+NR and HFpEF +NR groups. Mice were fed a 2-hit strategy diet or diet supplemented with NR; **H,** IPGTT was performed after 16 hours of fasting by injecting sterile 20% dextrose (2 g/kg) intraperitoneally; **I,** AUC was calculated using the trapezoidal rule for glucose levels from 0 to 120 min post-injection. Data presented as mean ± SEM ; each point represents an individual animal. Statistical Analysis based on the one-way ANOVA with Tukey's test.

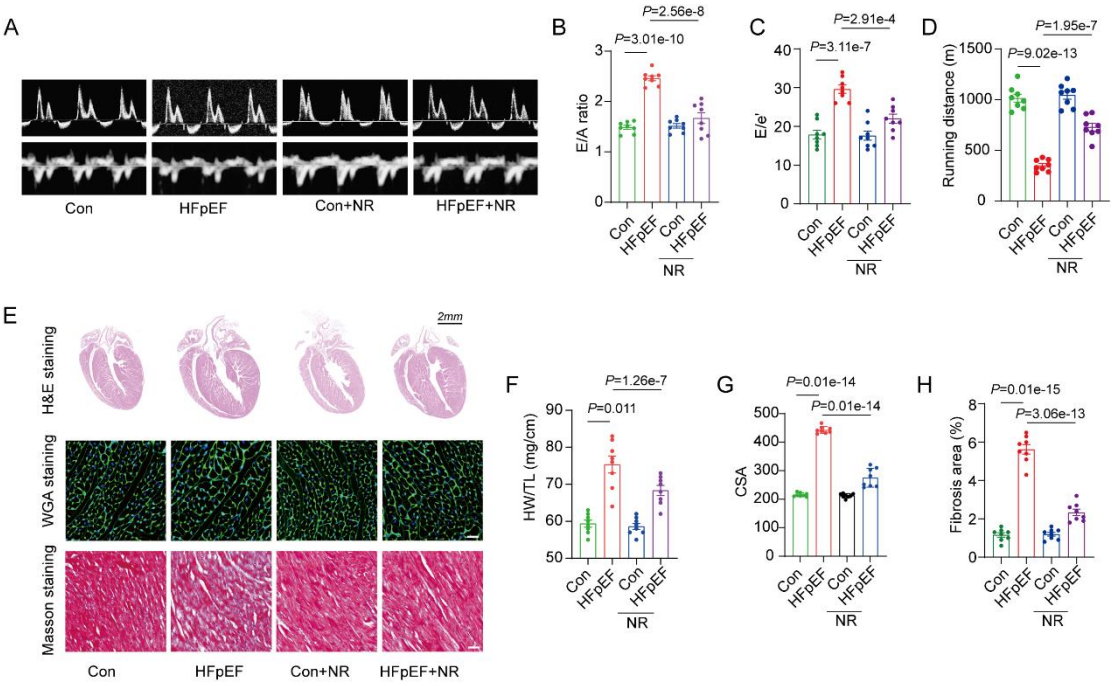

FigS6 NR supplementation prevented cardiac dysfunction and pathological remodeling in the HFpEF hearts.

A-C, Early to late diastolic transmitral flow velocity ratio (E/A) and early transmitral flow velocity to mitral annular early diastolic velocity ratio (E/e′) values were measured using echocardiography to assess cardiac diastolic function; **D**, Treadmill running distance was measured to assess exercise tolerance; **E**, Representative images of HE staining, WGA staining and Masson staining of the heart; **F,** ratio of heart weight (HW) to tibia length (TL); **G,** cardiomyocyte cross-sectional area (CSA) quantification; **H,** quantification of interstitial fibrosis area. Data presented as mean ± SEM; each point represents an independent biologic repeat; Statistical Analysis based on the one-way ANOVA with Tukey's test.

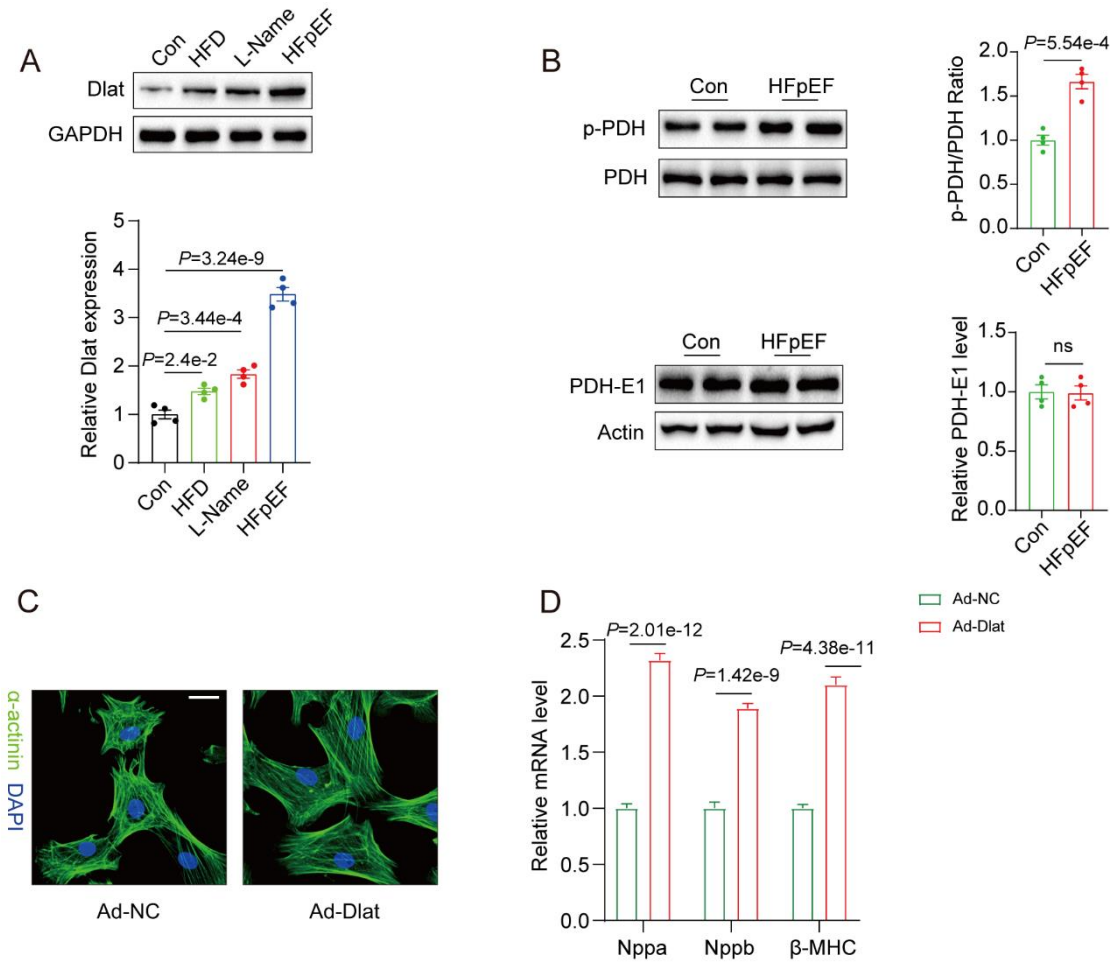

FigS7 Dlat overexpression induced pathological hypertrophy in NRVCMs.

A, Dlat expression were determined in the heart of HFD-fed, L-Name-fed and HFpEF mice; **B**, level of PDH and phosphorylated-PDH level were determined in the HFpEF hearts; **C,** Immunofluorescence for cytoskeletal (green) was performed to assess cardiomyocyte morphology; **D,** mRNA expression of Nppa, Nppb and β-MHC was measured by qRT-PCR in cardiomyocyte transfected with Ad-Dlat. Data presented as mean ± SEM; each point represents an independent biologic repeat; Statistical Analysis based on the two-way ANOVA test.

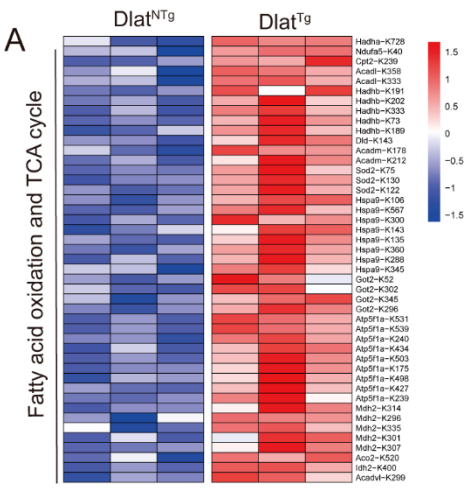

FigS8 Main proteins involved in TCA cycles and FAO were overacetylated in Dlat^{Tg} hearts.

A, Heatmap showing the acetylation levels of peptides mapping to TCA cycle and fatty acid oxidation in Dlat^{Tg} heart as compared to Dlat^{NTg} group (n=3 mice per group).

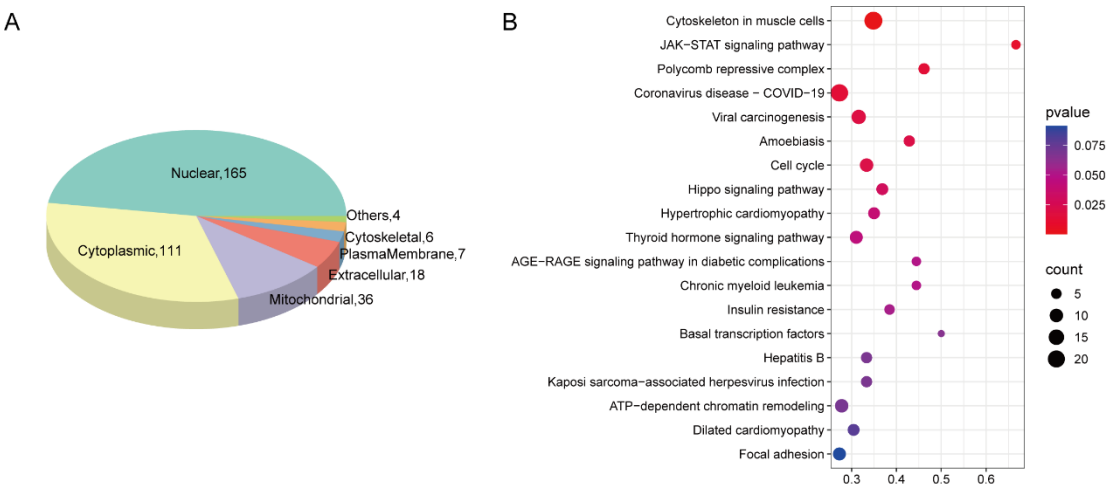

FigS9 Down-regulated acetylated proteins in the HFpEF hearts were analyzed by acetylome profiling.

A, Subcellular distribution of the down-regulate hyperacetylated proteins in Dlat^{Tg} hearts (n=3 mice per group); **B,** Kyoto Encyclopedia of Genes and Genomes (KEGG) enrichment analysis of the down-acetylated proteins in the Dlat^{Tg} hearts.

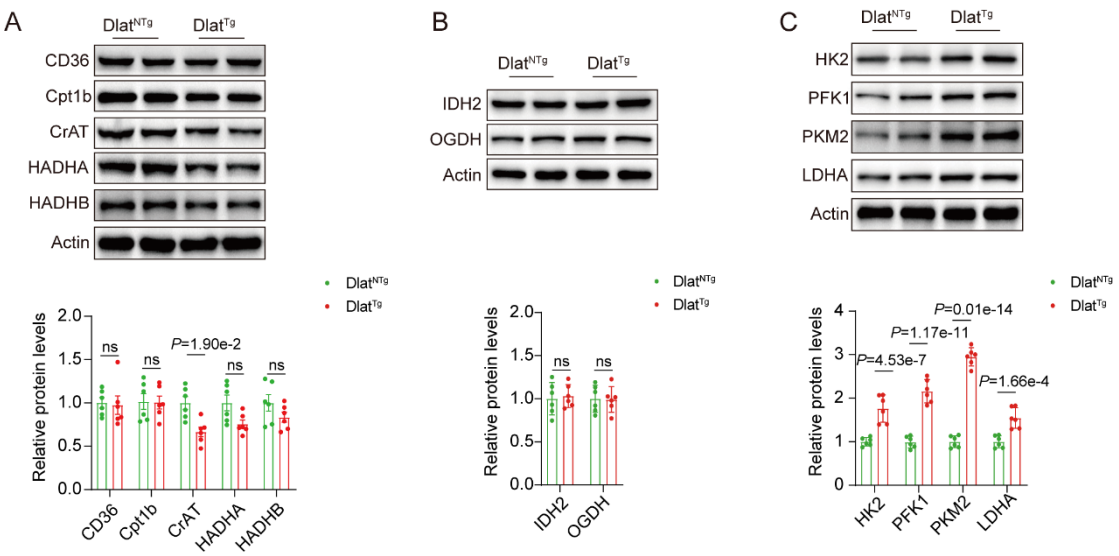

FigS10 Major proteins involved in FAO, TCA cycle and glycolysis were determined in the Dlat^{Tg} heart.

A, Protein levels of major FAO-related proteins CD36, Cpt1b, CrAT, HADHA, HADHB in Dlat^{Tg} and Dlat^{NTg} left ventricular tissues were analyzed by Western blot; **B,** Protein of key enzymes in TCA cycle IDH2 and OGDH expression levels were determined in Dlat^{Tg} and Dlat^{NTg} heart; **C,** Protein expression of key enzymes in the glycolytic HK2, PFK1, PKM2 and LDHA in Dlat^{Tg} and Dlat^{NTg} heart were examined. Data presented as mean ± SEM; each point represents an individual animal; Statistical Analysis based on the 2-way ANOVA.

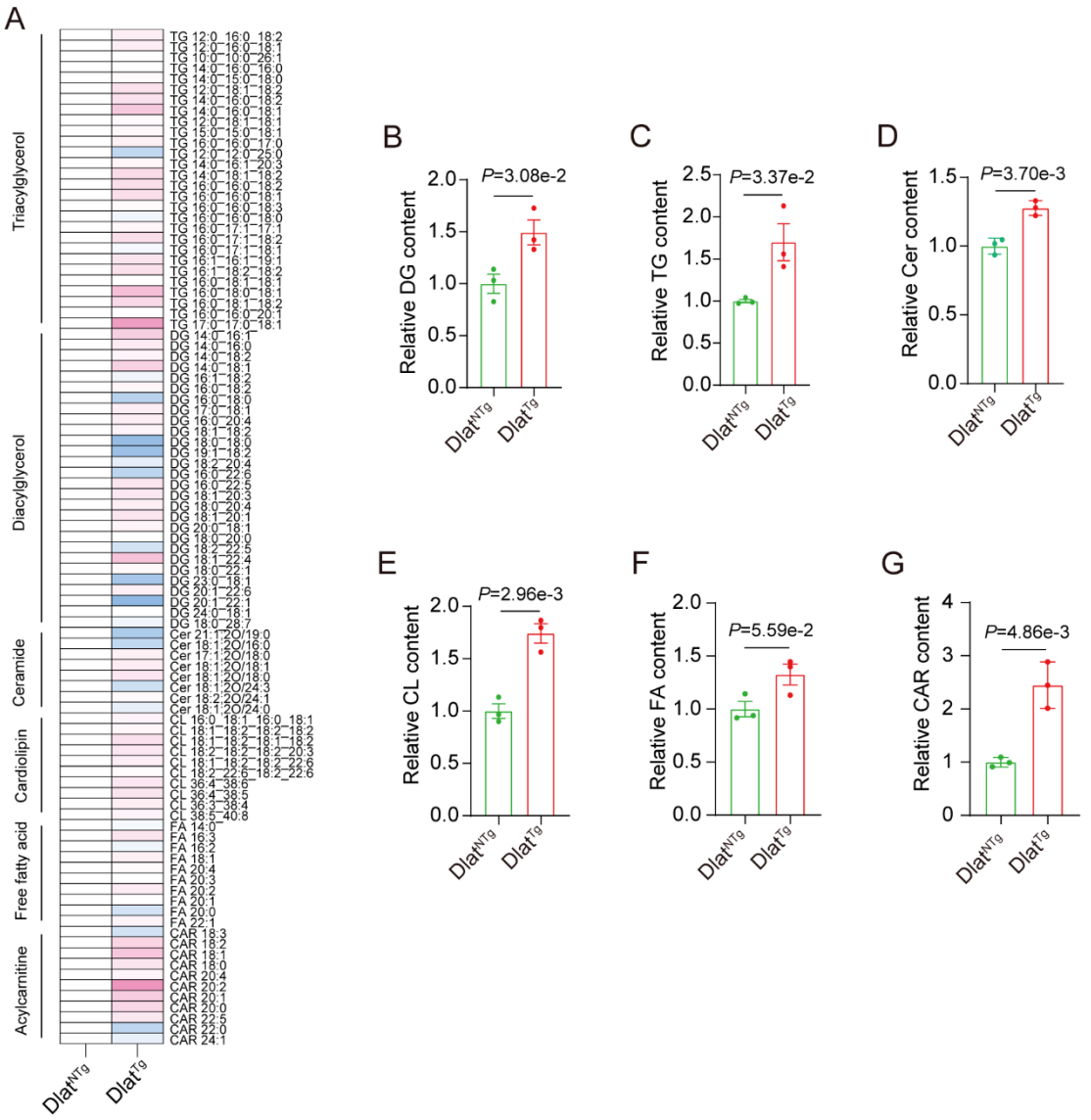

Fig S11. A lipidomic approach was used to examine the changes of lipid species in the heart tissue from the Dlat^{Tg} mice.

A, Lipidomics heatmap showing differentially expressed lipids in Dlat^{Tg} vs. Dlat^{NTg} mice. Rows represent individual lipids and columns represent biological replicates (n = 3 mice per group). **B,** Quantitative analysis of lipids content (n = 3 mice per group). Data presented as mean ± SEM; each point represents an individual animal; Statistical Analysis based on the Student's t-test.

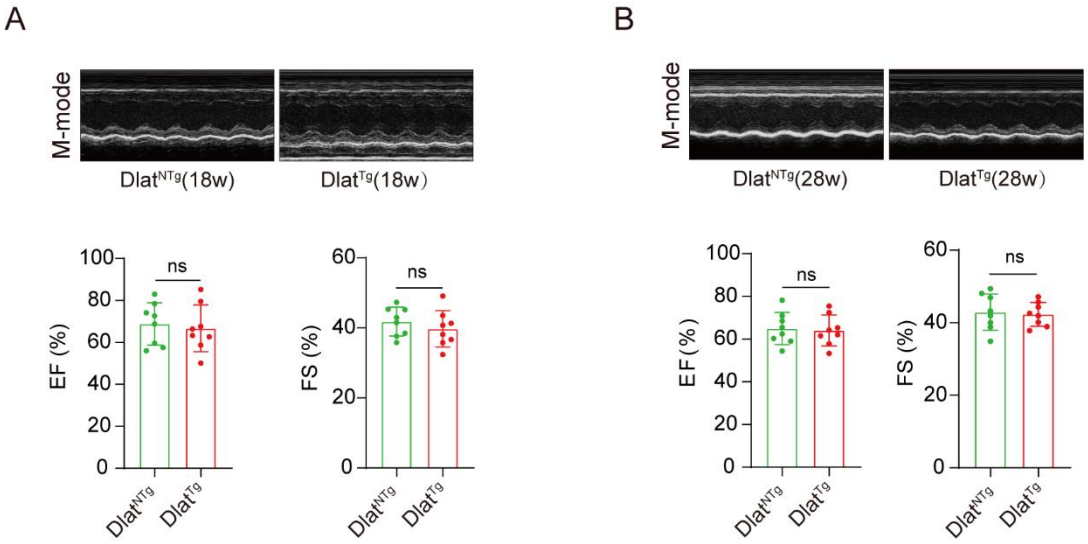

FigS12 Cardiac systolic function was determined in Dlat^{Tg} mice.

A-B, Left Ventricular Ejection Fraction (LVEF) and left ventricular fractional shortening (LVFS) values were measured using echocardiography to assess left ventricular systolic function at period of 18w and 28w in Dlat^{Tg} vs. Dlat^{NTg} mice (n = 8 mice per group). Data presented as mean ± SEM; each point represents an individual animal; Statistical Analysis based on the Student's t-test.

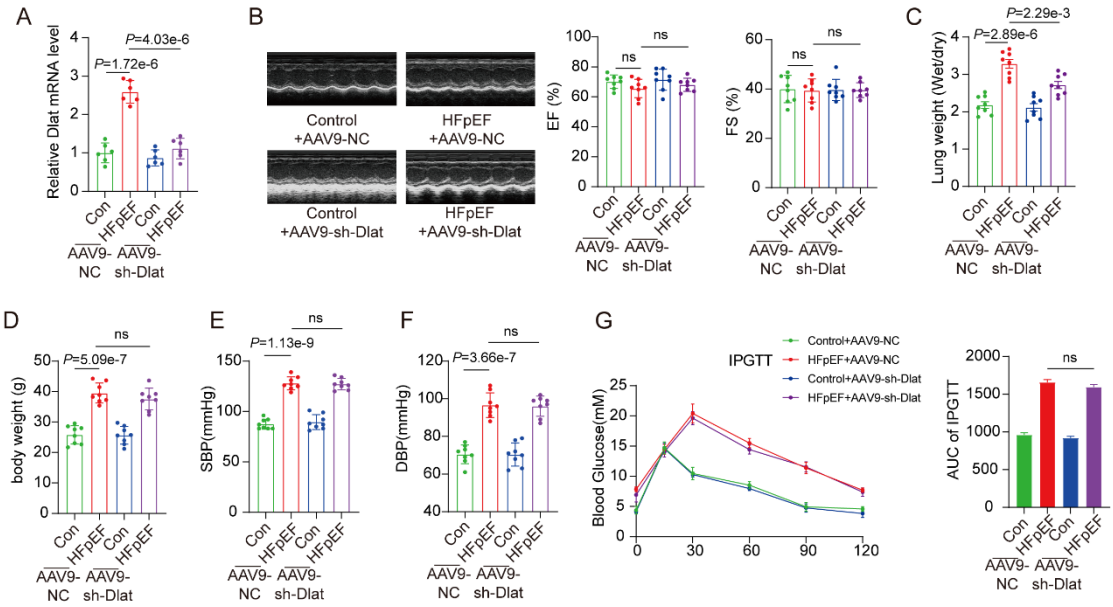

FigS13 Impact of AAV9-sh-Dlat injection on systemic comorbidities, cardiac systolic function, and glucose hemostasis in HFpEF mice.

A, mRNA expression of Dlat was measured by qRT-PCR from the control and HFpEF hearts transfected with AAV9-NC or AAV9-sh-Dlat**; B,** Left Ventricular Ejection Fraction(LVEF) and left ventricular fractional shortening (LVFS) values were measured using echocardiography to assess left ventricular systolic function; **C,** The ratio of wet-to-dry lung weight was using to assess pulmonary congestion; **D,** Body weight of male C57BL/6 mice in the control+AAV9-NC, HFpEF+AAV9-NC, control+AAV9-sh-Dlat and HFpEF+AAV9-sh-Dlat groups, Mice were fed a 2-hit strategy diet; **E-F,** Systolic blood pressures (SBP) and diastolic blood pressures (DBP) were recorded using a pressure transducer (AD Instruments); **G,** IPGTT was performed after 16 hours of fasting by injecting sterile 20% dextrose (2 g/kg) intraperitoneally, AUC was calculated using the trapezoidal rule for glucose levels from 0 to 120 min post-injection. Data presented as mean ± SEM ; each point represents an individual animal. Statistical Analysis based on the one-way ANOVA with Tukey's test.

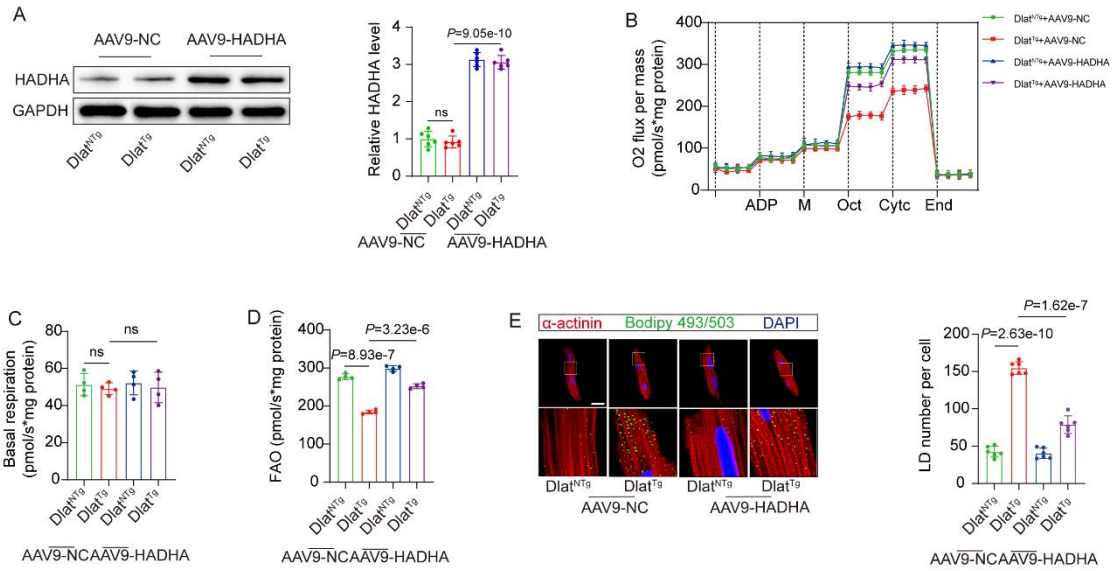

FigS14 Cardiac-specific HADHA overexpression restored cardiac FAO in Dlat^{Tg} mice.

A, Protein expression of HADHA from the Dlat^{NTg} and Dlat^{Tg} hearts transfected with AAV9-NC or AAV9-HADHA was examined. **B,** Respirational flux of cardiac tissue was determined using an Oroboros clark-type electrode (n=4 biological replicates); **C,** Basic respiratory measured by oxygen consumption; **D,** FAO measured by oxygen consumption; **E,** Intra-myocardial lipid droplet (LD) was determined by Bodipy 493/503 staining in isolated adult cardiomyocytes and the number of LDs per cell were quantified (n=10 biological replicates). Data presented as mean ± SEM; each point represents an individual animal; Statistical Analysis based on the one-way ANOVA with Tukey's test.

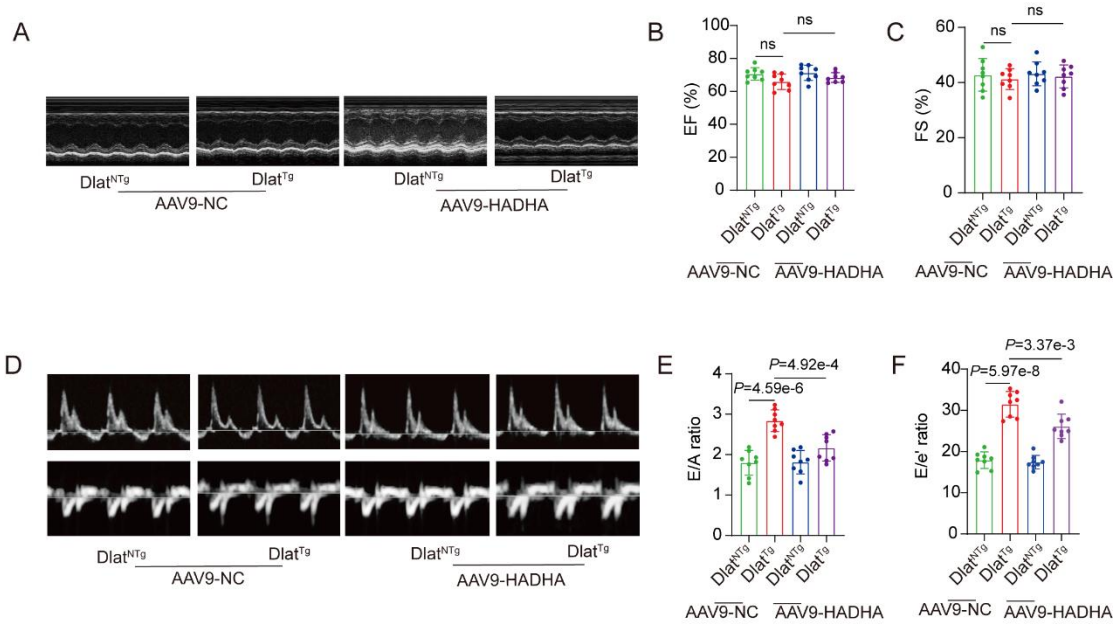

FigS15 Cardiac-specific HADHA overexpression mitigated cardiac dysfunction in Dlat^{Tg} mice.

A-C, Left Ventricular Ejection Fraction (LVEF) and left ventricular fractional shortening (LVFS) values were measured using echocardiography to assess left ventricular systolic function; **D-F,** Early to late diastolic transmitral flow velocity ratio (E/A) and early transmitral flow velocity to mitral annular early diastolic velocity ratio (E/e′) values were measured using echocardiography to assess cardiac diastolic function. Data presented as mean ± SEM ; each point represents an individual animal. Statistical Analysis based on the one-way ANOVA with Tukey's test.

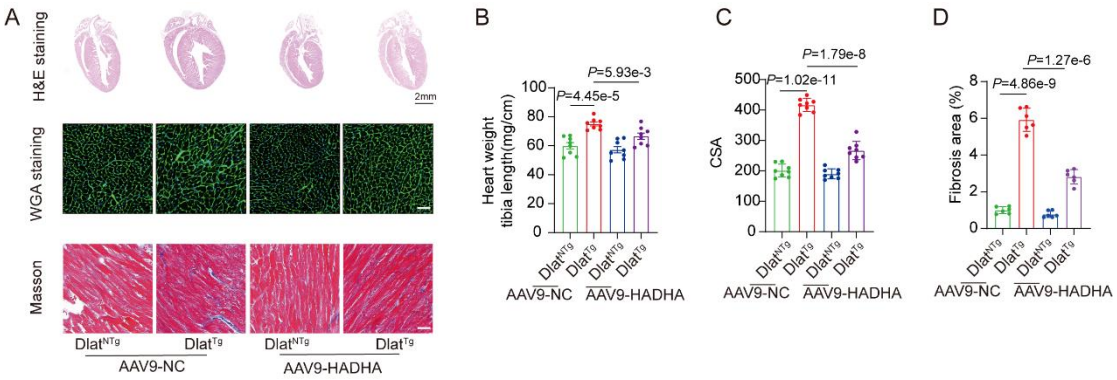

FigS16 Cardiac-specific HADHA overexpression ameliorated cardiac pathological changes in Dlat^{Tg} mice.

A, Representative images of Hematoxylin-eosin (HE) staining, immunohistochemistry for wheat germ agglutinin (WGA) staining of the left ventricle, and using Masson trichrome staining for assess interstitial fibrosis; **B,** Ratio of heart weight (HW) to tibia length; **C,** Immunohistochemistry for wheat germ agglutinin (WGA) staining of the left ventricle; **D,** Quantification of interstitial fibrosis area. Data presented as mean ± SEM ; each point represents an individual animal. Statistical Analysis based on the one-way ANOVA with Tukey's test.

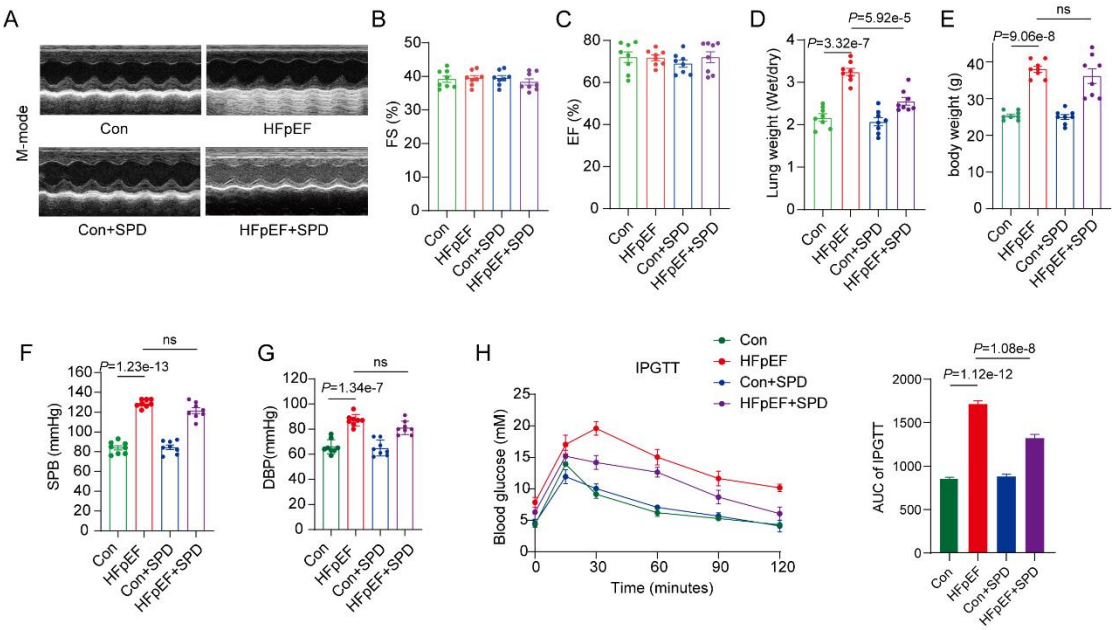

FigS17 Impact of SPD supplementation on systemic comorbidities, cardiac systolic function, and glucose hemostasis in HFpEF mice.

A-C, Left Ventricular Ejection Fraction(LVEF) and left ventricular fractional shortening (LVFS) values were measured using echocardiography to assess left ventricular systolic function; **D,** The ratio of wet-to-dry lung weight was using to assess pulmonary congestion; **E,** Body weight of male C57BL/6 mice in the control, HFpEF, control+SPD and HFpEF +SPD groups, Mice were fed a 2-hit strategy diet or diet supplemented with SPD; **F-G,** Systolic blood pressures (SBP) and diastolic blood pressures (DBP) were recorded using a pressure transducer (AD Instruments); **H,** IPGTT was performed after 16 hours of fasting by injecting sterile 20% dextrose (2 g/kg) intraperitoneally, AUC was calculated using the trapezoidal rule for glucose levels from 0 to 120 min post-injection. Data presented as mean ± SEM ; each point represents an individual animal. Statistical Analysis based on the one-way ANOVA with Tukey's test.